

**Azimuthal Anisotropy and Correlations at Large Transverse Momenta
in $p + p$ and Au + Au Collisions at $\sqrt{s_{NN}} = 200$ GeV**

- J. Adams,³ M. M. Aggarwal,²⁹ Z. Ahammed,⁴³ J. Amonett,²⁰ B. D. Anderson,²⁰ D. Arkhipkin,¹³ G. S. Averichev,¹²
 S. K. Badyal,¹⁹ Y. Bai,²⁷ J. Balewski,¹⁷ O. Barannikova,³² L. S. Barnby,³ J. Baudot,¹⁸ S. Bekele,²⁸ V. V. Belaga,¹²
 R. Bellwied,⁴⁶ J. Berger,¹⁴ B. I. Bezverkhny,⁴⁸ S. Bharadwaj,³³ A. Bhasin,¹⁹ A. K. Bhati,²⁹ V. S. Bhatia,²⁹ H. Bichsel,⁴⁵
 A. Billmeier,⁴⁶ L. C. Bland,⁴ C. O. Blyth,³ B. E. Bonner,³⁴ M. Botje,²⁷ A. Boucham,³⁸ A. V. Brandin,²⁵ A. Bravar,⁴
 M. Bystersky,¹¹ R. V. Cadman,¹ X. Z. Cai,³⁷ H. Caines,⁴⁸ M. Calderón de la Barca Sánchez,⁴ J. Carroll,²¹ J. Castillo,²¹
 D. Cebrá,⁷ Z. Chajecki,⁴⁴ P. Chaloupka,¹¹ S. Chattopadhyay,⁴³ H. F. Chen,³⁶ Y. Chen,⁸ J. Cheng,⁴¹ M. Cherney,¹⁰
 A. Chikanian,⁴⁸ W. Christie,⁴ J. P. Coffin,¹⁸ T. M. Cormier,⁴⁶ J. G. Cramer,⁴⁵ H. J. Crawford,⁶ D. Das,⁴³ S. Das,⁴³
 M. M. de Moura,³⁵ A. A. Derevschikov,³¹ L. Didenko,⁴ T. Dietel,¹⁴ S. M. Dogra,¹⁹ W. J. Dong,⁸ X. Dong,³⁶ J. E. Draper,⁷
 F. Du,⁴⁸ A. K. Dubey,¹⁵ V. B. Dunin,¹² J. C. Dunlop,⁴ M. R. Dutta Mazumdar,⁴³ V. Eckardt,²³ W. R. Edwards,²¹
 L. G. Efimov,¹² V. Emelianov,²⁵ J. Engelage,⁶ G. Eppley,³⁴ B. Erazmus,³⁸ M. Estienne,³⁸ P. Fachini,⁴ J. Faivre,¹⁸
 R. Fatemi,¹⁷ J. Fedorisin,¹² K. Filimonov,²¹ P. Filip,¹¹ E. Finch,⁴⁸ V. Fine,⁴ Y. Fisyak,⁴ K. J. Foley,⁴ K. Fomenko,¹² J. Fu,⁴¹
 C. A. Gagliardi,³⁹ J. Gans,⁴⁸ M. S. Ganti,⁴³ L. Gaudichet,³⁸ F. Geurts,³⁴ V. Ghazikhanian,⁸ P. Ghosh,⁴³ J. E. Gonzalez,⁸
 O. Grachov,⁴⁶ O. Grebenyuk,²⁷ D. Grosnick,⁴² S. M. Guertin,⁸ Y. Guo,⁴⁶ A. Gupta,¹⁹ T. D. Gutierrez,⁷ T. J. Hallman,⁴
 A. Hamed,⁴⁶ D. Hardtke,²¹ J. W. Harris,⁴⁸ M. Heinz,² T. W. Henry,³⁹ S. Hepplemann,³⁰ B. Hippolyte,⁴⁸ A. Hirsch,³²
 E. Hjort,²¹ G. W. Hoffmann,⁴⁰ H. Z. Huang,⁸ S. L. Huang,³⁶ E. W. Hughes,⁵ T. J. Humanic,²⁸ G. Igo,⁸ A. Ishihara,⁴⁰
 P. Jacobs,²¹ W. W. Jacobs,¹⁷ M. Janik,⁴⁴ H. Jiang,⁸ P. G. Jones,³ E. G. Judd,⁶ S. Kabana,² K. Kang,⁴¹ M. Kaplan,⁹
 D. Keane,²⁰ V. Yu. Khodyrev,³¹ J. Kiryluk,²² A. Kisiel,⁴⁴ E. M. Kislov,¹² J. Klay,²¹ S. R. Klein,²¹ A. Klyachko,¹⁷
 D. D. Koetke,⁴² T. Kollegger,¹⁴ M. Kopytine,²⁰ L. Kotchenda,²⁵ M. Kramer,²⁶ P. Kravtsov,²⁵ V. I. Kravtsov,³¹ K. Krueger,¹
 C. Kuhn,¹⁸ A. I. Kulikov,¹² A. Kumar,²⁹ C. L. Kunz,⁹ R. Kh. Kutuev,¹³ A. A. Kuznetsov,¹² M. A. C. Lamont,⁴⁸
 J. M. Landgraf,⁴ S. Lange,¹⁴ F. Laue,⁴ J. Lauret,⁴ A. Lebedev,⁴ R. Lednický,¹² S. Lehocká,¹² M. J. LeVine,⁴ C. Li,³⁶ Q. Li,⁴⁶
 Y. Li,⁴¹ S. J. Lindenbaum,²⁶ M. A. Lisa,²⁸ F. Liu,⁴⁷ L. Liu,⁴⁷ Q. J. Liu,⁴⁵ Z. Liu,⁴⁷ T. Ljubicic,⁴ W. J. Llope,³⁴ H. Long,⁸
 R. S. Longacre,⁴ M. Lopez-Noriega,²⁸ W. A. Love,⁴ Y. Lu,⁴⁷ T. Ludlam,⁴ D. Lynn,⁴ G. L. Ma,³⁷ J. G. Ma,⁸ Y. G. Ma,³⁷
 D. Magestro,²⁸ S. Mahajan,¹⁹ D. P. Mahapatra,¹⁵ R. Majka,⁴⁸ L. K. Mangotra,¹⁹ R. Manweiler,⁴² S. Margetis,²⁰
 C. Markert,⁴⁸ L. Martin,³⁸ J. N. Marx,²¹ H. S. Matis,²¹ Yu. A. Matulenko,³¹ C. J. McClain,¹ T. S. McShane,¹⁰ F. Meissner,²¹
 Yu. Melnick,³¹ A. Meschanin,³¹ M. L. Miller,²² Z. Milosevich,⁹ N. G. Minaev,³¹ C. Mironov,²⁰ A. Mischke,²⁷
 D. K. Mishra,¹⁵ J. Mitchell,³⁴ B. Mohanty,⁴³ L. Molnar,³² C. F. Moore,⁴⁰ D. A. Morozov,³¹ M. G. Munhoz,³⁵ B. K. Nandi,⁴³
 S. K. Nayak,¹⁹ T. K. Nayak,⁴³ J. M. Nelson,³ P. K. Netrakanti,⁴³ V. A. Nikitin,¹³ L. V. Nogach,³¹ S. B. Nurushev,³¹
 G. Odyniec,²¹ A. Ogawa,⁴ V. Okorokov,²⁵ M. Oldenburg,²¹ D. Olson,²¹ S. K. Pal,⁴³ Y. Panebratsev,¹² S. Y. Panitkin,⁴
 A. I. Pavlinov,⁴⁶ T. Pawlak,⁴⁴ T. Peitzmann,²⁷ V. Perevoztchikov,⁴ C. Perkins,⁶ W. Peryt,⁴⁴ V. A. Petrov,¹³ S. C. Phatak,¹⁵
 R. Picha,⁷ M. Planinic,⁴⁹ J. Pluta,⁴⁴ N. Porile,³² J. Porter,⁴⁵ A. M. Poskanzer,²¹ M. Potekhin,⁴ E. Potrebenikova,¹²
 B. V. K. S. Potukuchi,¹⁹ D. Prindle,⁴⁵ C. Pruneau,⁴⁶ J. Putschke,²³ G. Rai,²¹ G. Rakness,³⁰ R. Raniwala,³³ S. Raniwala,³³
 O. Ravel,³⁸ R. L. Ray,⁴⁰ S. V. Razin,¹² D. Reichhold,³² J. G. Reid,⁴⁵ G. Renault,³⁸ F. Retiere,²¹ A. Ridiger,²⁵ H. G. Ritter,²¹
 J. B. Roberts,³⁴ O. V. Rogachevskiy,¹² J. L. Romero,⁷ A. Rose,⁴⁶ C. Roy,³⁸ L. Ruan,³⁶ R. Sahoo,¹⁵ I. Sakrejda,²¹ S. Salur,⁴⁸
 J. Sandweiss,⁴⁸ I. Savin,¹³ P. S. Sazhin,¹² J. Schambach,⁴⁰ R. P. Scharenberg,³² N. Schmitz,²³ L. S. Schroeder,²¹
 K. Schweda,²¹ J. Seger,¹⁰ P. Seyboth,²³ E. Shahaliev,¹² M. Shao,³⁶ W. Shao,⁵ M. Sharma,²⁹ W. Q. Shen,³⁷
 K. E. Shesternov,³¹ S. S. Shimanskiy,¹² E. Sichtermann,²¹ F. Simon,²³ R. N. Singaraju,⁴³ G. Skoro,¹² N. Smirnov,⁴⁸
 R. Snellings,²⁷ G. Sood,⁴² P. Sorensen,²¹ J. Sowinski,¹⁷ J. Speltz,¹⁸ H. M. Spinka,¹ B. Srivastava,³² A. Stadnik,¹²
 T. D. S. Stanislaus,⁴² R. Stock,¹⁴ A. Stolpovsky,⁴⁶ M. Strikhanov,²⁵ B. Stringfellow,³² A. A. P. Suaide,³⁵ E. Sugarbaker,²⁸
 C. Suire,⁴ M. Sumbera,¹¹ B. Surrow,²² T. J. M. Symons,²¹ A. Szanto de Toledo,³⁵ P. Szarwas,⁴⁴ A. Tai,⁸ J. Takahashi,³⁵
 A. H. Tang,²⁷ T. Tarnowsky,³² D. Thein,⁸ J. H. Thomas,²¹ S. Timoshenko,²⁵ M. Tokarev,¹² S. Trentalange,⁸ R. E. Tribble,³⁹
 O. D. Tsai,⁸ J. Ulery,³² T. Ullrich,⁴ D. G. Underwood,¹ A. Urkinbaev,¹² G. Van Buren,⁴ M. van Leeuwen,²¹
 A. M. Vander Molen,²⁴ R. Varma,¹⁶ I. M. Vasilevski,¹³ A. N. Vasiliev,³¹ R. Vernet,¹⁸ S. E. Vigdor,¹⁷ Y. P. Viyogi,⁴³
 S. Vokal,¹² S. A. Voloshin,⁴⁶ M. Vznuzdaev,²⁵ W. T. Waggoner,¹⁰ F. Wang,³² G. Wang,²⁰ G. Wang,⁵ X. L. Wang,³⁶
 Y. Wang,⁴⁰ Y. Wang,⁴¹ Z. M. Wang,³⁶ H. Ward,⁴⁰ J. W. Watson,²⁰ J. C. Webb,¹⁷ R. Wells,²⁸ G. D. Westfall,²⁴ A. Wetzler,²¹
 C. Whitten, Jr.,⁸ H. Wieman,²¹ S. W. Wissink,¹⁷ R. Witt,² J. Wood,⁸ J. Wu,³⁶ N. Xu,²¹ Z. Xu,⁴ Z. Z. Xu,³⁶ E. Yamamoto,²¹
 P. Yepes,³⁴ V. I. Yurevich,¹² Y. V. Zanevsky,¹² H. Zhang,⁴ W. M. Zhang,²⁰ Z. P. Zhang,³⁶ P. A. Zolnierczuk,¹⁷
 R. Zoukarneev,¹³ Y. Zoukarneeva,¹³ and A. N. Zubarev¹²

(STAR Collaboration)

- ¹Argonne National Laboratory, Argonne, Illinois 60439, USA
²University of Bern, 3012 Bern, Switzerland
³University of Birmingham, Birmingham, United Kingdom
⁴Brookhaven National Laboratory, Upton, New York 11973, USA
⁵California Institute of Technology, Pasadena, California 91125, USA
⁶University of California, Berkeley, California 94720, USA
⁷University of California, Davis, California 95616, USA
⁸University of California, Los Angeles, California 90095, USA
⁹Carnegie Mellon University, Pittsburgh, Pennsylvania 15213, USA
¹⁰Creighton University, Omaha, Nebraska 68178, USA
¹¹Nuclear Physics Institute AS CR, 250 68 Řež/Prague, Czech Republic
¹²Laboratory for High Energy (JINR), Dubna, Russia
¹³Particle Physics Laboratory (JINR), Dubna, Russia
¹⁴University of Frankfurt, Frankfurt, Germany
¹⁵Institute of Physics, Bhubaneswar 751005, India
¹⁶Indian Institute of Technology, Mumbai, India
¹⁷Indiana University, Bloomington, Indiana 47408, USA
¹⁸Institut de Recherches Subatomiques, Strasbourg, France
¹⁹University of Jammu, Jammu 180001, India
²⁰Kent State University, Kent, Ohio 44242, USA
²¹Lawrence Berkeley National Laboratory, Berkeley, California 94720, USA
²²Massachusetts Institute of Technology, Cambridge, Massachusetts 02139-4307, USA
²³Max-Planck-Institut für Physik, Munich, Germany
²⁴Michigan State University, East Lansing, Michigan 48824, USA
²⁵Moscow Engineering Physics Institute, Moscow, Russia
²⁶City College of New York, New York City, New York 10031, USA
²⁷NIKHEF, Amsterdam, The Netherlands
²⁸The Ohio State University, Columbus, Ohio 43210, USA
²⁹Panjab University, Chandigarh 160014, India
³⁰Pennsylvania State University, University Park, Pennsylvania 16802, USA
³¹Institute of High Energy Physics, Protvino, Russia
³²Purdue University, West Lafayette, Indiana 47907, USA
³³University of Rajasthan, Jaipur 302004, India
³⁴Rice University, Houston, Texas 77251, USA
³⁵Universidade de São Paulo, São Paulo, Brazil
³⁶University of Science & Technology of China, Anhui 230027, China
³⁷Shanghai Institute of Applied Physics, Shanghai 201800, China
³⁸SUBATECH, Nantes, France
³⁹Texas A&M University, College Station, Texas 77843, USA
⁴⁰University of Texas, Austin, Texas 78712, USA
⁴¹Tsinghua University, Beijing 100084, China
⁴²Valparaiso University, Valparaiso, Indiana 46383, USA
⁴³Variable Energy Cyclotron Centre, Kolkata 700064, India
⁴⁴Warsaw University of Technology, Warsaw, Poland
⁴⁵University of Washington, Seattle, Washington 98195, USA
⁴⁶Wayne State University, Detroit, Michigan 48201, USA
⁴⁷Institute of Particle Physics, CCNU (HZNU), Wuhan 430079, China
⁴⁸Yale University, New Haven, Connecticut 06520, USA
⁴⁹University of Zagreb, Zagreb, HR-10002, Croatia

(Received 9 July 2004; published 15 December 2004)

Results on high transverse momentum charged particle emission with respect to the reaction plane are presented for Au + Au collisions at $\sqrt{s_{NN}} = 200$ GeV. Two- and four-particle correlations results are presented as well as a comparison of azimuthal correlations in Au + Au collisions to those in $p + p$ at the same energy. The elliptic anisotropy v_2 is found to reach its maximum at $p_t \sim 3$ GeV/c, then decrease slowly and remain significant up to $p_t \approx 7\text{--}10$ GeV/c. Stronger suppression is found in the back-to-back high- p_t particle correlations for particles emitted out of plane compared to those emitted in plane. The centrality dependence of v_2 at intermediate p_t is compared to simple models based on jet quenching.

In high energy heavy-ion collisions, a high density system consisting of deconfined quarks and gluons is expected to be created [1]. Energetic partons, resulting from initial hard scatterings, are predicted to lose energy by induced gluon radiation when propagating through the medium [2]. This energy loss is expected to depend strongly on the color charge density of the created system and the traversed path length of the propagating parton. At Brookhaven's Relativistic Heavy-Ion Collider (RHIC) three different observations related to parton energy loss have emerged: strong suppression of the inclusive hadron production [3–5], strong suppression of the back-to-back high- p_t jetlike correlation [6,7], and large values of the elliptic flow at high p_t [8]. In noncentral heavy-ion collisions, the geometrical overlap region has an almond shape in the transverse plane, with its short axis in the reaction plane. Depending on the emission azimuthal angle, partons traversing this system, on average, experience different path lengths and therefore different energy loss. It leads to (a) azimuthal anisotropy in high p_t particle production with respect to the reaction plane [9,10] [the second harmonic in the particle azimuthal distribution, elliptic flow, is characterized [11] by $v_2 = \langle \cos(2(\phi - \Psi_R)) \rangle$], and (b) to the dependence of the high p_t two-particle back-to-back correlations on the orientation of the pair.

In this Letter, using higher-order cumulant analysis [12,13] and comparing azimuthal correlations measured in $p + p$ collisions to those in Au + Au, we confirm strong elliptic flow in midcentral Au + Au collisions at least up to $p_t \approx 7$ GeV/c as qualitatively expected in the jet-quenching scenario. We further investigate the influence of the jet-quenching mechanism on high- p_t particle production with respect to the reaction plane by studying v_2 centrality dependence in the intermediate p_t region and two-particle azimuthal correlations at different angles with respect to the reaction plane.

The data set consists of about 2×10^6 minimum bias and 1.2×10^6 central trigger Au + Au events and 11×10^6 $p + p$ events at $\sqrt{s_{NN}} = 200$ GeV. The measurements were made using the Time Projection Chamber [14] of the STAR detector [15], which covers pseudorapidity (η) from -1.3 to 1.3 . The event centrality in this Letter is defined by the multiplicity measured at midrapidity by STAR [4]. Tracks used to reconstruct the flow vector, or generating function [13] in the case of the cumulant method, were subject to the same quality cuts as used in the $\sqrt{s_{NN}} = 130$ GeV analysis [16,17], except for the low transverse momentum cutoff, which for this analysis is 0.15 GeV/c instead of 0.10 GeV/c.

One of the largest uncertainties in elliptic flow measurements in nuclear collisions is due to so-called nonflow effects—the contribution to the azimuthal correlations not related to the reaction plane orientation, such as resonance decays and interjet and intrajet correlations. The

importance of these effects can be investigated by comparing the azimuthal correlations measured in Au + Au to those in $p + p$ collisions, where all correlations are considered to be of nonflow origin. For such a comparison we evaluate the accumulative correlation of a particle from a given p_t bin with all other particles in the region $0.15 < p_t < 2.0$ GeV/c and $|\eta| < 1.0$ by calculating the event average sum:

$$\left\langle \sum_i \cos(2(\phi_{p_t} - \phi_i)) \right\rangle = M v_2(p_t) \bar{v}_2 + \{\text{nonflow}\}, \quad (1)$$

where ϕ_{p_t} is the azimuthal angle of the particle from a given p_t bin. The first term in the right-hand side of Eq. (1) represents the elliptic flow contribution, where $v_2(p_t)$ is the elliptic flow of particles with a given p_t , and \bar{v}_2 is the average flow of particles used in the sum; M is the multiplicity of particles contributing to the sum. The multiplicity in the sum changes with the centrality of the collision, but as long as the relative number of particles (per trigger particle) involved in nonflow effects does not change, the contribution due to these effects is a constant. Comparing $p + p$ and Au + Au collisions, one indeed might expect some changes in particle correlations: there could be an increase in correlations due to a possible increase of jet multiplicities in Au + Au collisions or, conversely, some decrease due to the suppression of high p_t back-to-back correlations [6]. It is difficult to make an accurate estimate of possible modifications of nonflow effects. The fact that at very high p_t the $p + p$ results are very close to central Au + Au (shown later by Fig. 1) suggests that the modifications are relatively small.

Figure 1 shows the azimuthal correlation, Eq. (1), as a function of transverse momentum for three different centrality ranges in Au + Au collisions, as compared to mini-

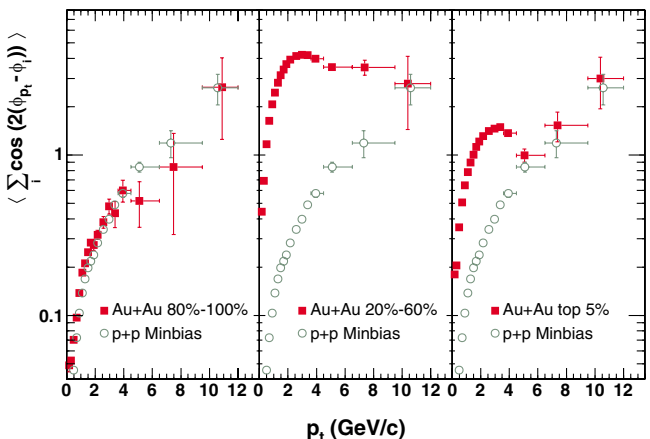


FIG. 1 (color online). Azimuthal correlations in Au + Au collisions (squares) as a function of centrality (peripheral to central from left to right) compared to minimum bias azimuthal correlations in $p + p$ collisions (circles). Errors are statistical only.

mum bias $p + p$ collisions. We observe that for the most peripheral Au + Au collisions, the azimuthal correlations are very similar to minimum bias $p + p$. In midcentral Au + Au events, the azimuthal correlations are very different from those in $p + p$ collisions in both magnitude and p_t dependence. Note that at $p_t = 7$ GeV/c, the azimuthal correlations in Au + Au collisions are still many standard deviations away from those observed in $p + p$ collisions, indicating significant elliptic flow up to these momenta. For the most central Au + Au collisions, at low p_t the magnitude of the correlations is also different from $p + p$. However, for particles with $p_t \geq 5$ GeV/c, the correlation in Au + Au collisions starts to follow that in $p + p$ collisions, suggesting that azimuthal correlations become dominated by nonflow effects and that the latter are rather similar in $p + p$ and Au + Au collisions at those momenta. The observed nonmonotonic centrality dependence of the azimuthal correlation at low and moderate p_t is strong evidence of elliptic flow. It is qualitatively different from that expected from intrajet correlations among jet fragments [18].

We also perform a multiparticle cumulant analysis, which is much less sensitive to nonflow effects than the traditional approach based on two-particle correlations. Figure 2 shows v_2 as a function of transverse momentum for 20%–60% of the total cross section. The v_2 obtained using the four-particle cumulant method, $v_2\{4\}$, is up to about 20% lower than the value of v_2 obtained from the two-particle cumulant method. This difference could be partially explained by nonflow effects, which are greatly suppressed in $v_2\{4\}$, and by the fluctuation of v_2 itself [17,19]. Flow fluctuations contribute to $v_2\{2\}$ and $v_2\{4\}$ with different signs. The true v_2 lies between $v_2\{4\}$ and approximately the average of $v_2\{2\}$ and $v_2\{4\}$. The systematic uncertainty is given by these two bounds. For the

centrality range plotted in Fig. 2, we find significant v_2 at least up to $p_t \approx 7$ GeV/c, well within the region where particle production is expected to be dominated by parton fragmentation. Two-particle cumulant results extend to 12 GeV/c, although at high p_t these might be dominated by nonflow contributions. Also shown in Fig. 2 by open circles are the two-particle correlation results after subtracting the correlations measured in $p + p$ collisions. The comparison of these results to $v_2\{4\}$ in the region $p_t < 4$ GeV/c indicates that either the relative contribution of nonflow effects is larger in Au + Au collisions compared to $p + p$, or there is a significant flow fluctuation contribution that would increase the apparent $v_2\{2\}$ values and decrease $v_2\{4\}$. In general, we observe that $v_2(p_t)$ reaches a maximum at about 3 GeV/c, confirming results obtained by PHENIX [20], and then slowly decreases.

The energy loss mechanism that leads to azimuthal anisotropy at high p_t also leads to a distinct feature in two-particle azimuthal correlations. At high transverse momenta, two-particle distributions in the relative azimuthal angle measured in $p + p$, $d + \text{Au}$, and Au + Au collisions at RHIC [6–8] exhibit a jetlike correlation characterized by the peaks at $\Delta\phi = 0$ (nearside correlations) and at $\Delta\phi = \pi$ (back-to-back). The back-to-back peak is found to be strongly suppressed in central Au + Au collisions [6]. In noncentral collisions, the suppression should depend on the relative orientation of the back-to-back pair with respect to the reaction plane. In the analysis of the two-particle azimuthal correlations, we select *trigger* particles with $4 < p_t^{\text{trig}} < 6$ GeV/c emitted in the direction of the event plane angle Ψ_2 (in plane, $|\phi^{\text{trig}} - \Psi_2| < \pi/4$ and $|\phi^{\text{trig}} - \Psi_2| > 3\pi/4$) and perpendicular to it (out of plane, $\pi/4 < |\phi^{\text{trig}} - \Psi_2| < 3\pi/4$). The trigger particles are paired with *associated* particles satisfying $2 \text{ GeV}/c < p_t < p_t^{\text{trig}}$. The tracks are restricted to $|\eta| < 1$. To reduce the effect of particles produced within a jet on the reaction plane reconstruction, all particles in a pseudorapidity region $|\Delta\eta| < 0.5$ around the highest p_t particle in the event are excluded from the event plane determination. In the upper panel of Fig. 3 we show the azimuthal distributions of associated particles for trigger particles that are in plane (squares) and out of plane (triangles) in midcentral Au + Au collisions. The distributions are corrected for the reconstruction efficiency. The measured distributions exhibit a strong elliptic flow pattern similar to that found in the recent analysis at the CERN Super Proton Synchrotron [21].

In the presence of elliptic flow the in-plane and out-of-plane two-particle azimuthal distributions are given by [22]

$$\frac{dn_{\text{out}}^{\text{in}}}{d\Delta\phi} = B \left[1 + 2v_2^{\text{assoc}} \frac{\pi v_2^{\text{trig}} \pm 2\langle \cos(2\Delta\Psi) \rangle}{\pi \pm 4v_2^{\text{trig}} \langle \cos(2\Delta\Psi) \rangle} \right] \times \cos(2\Delta\phi), \quad (2)$$

where v_2^{assoc} and v_2^{trig} are the elliptic flow of the associated

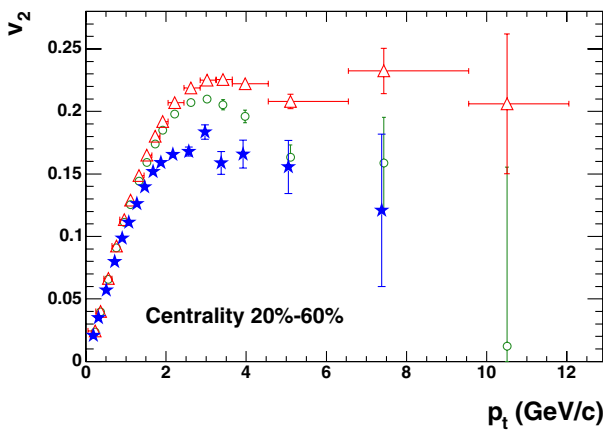


FIG. 2 (color online). v_2 of charged particles as a function of transverse momentum from the two-particle cumulant method (triangles) and four-particle cumulant method (stars). Open circles show the two-particle correlation results after subtracting the correlations measured in $p + p$ collisions. Only statistical errors are shown.

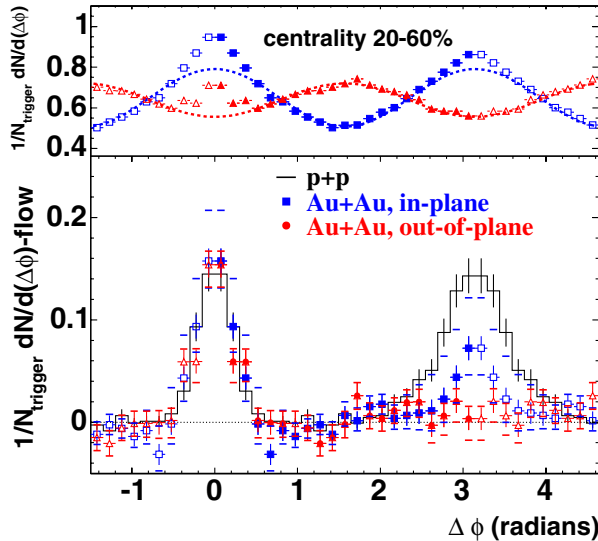


FIG. 3 (color online). Upper panel: Azimuthal distributions of associated particles for trigger particles in plane (squares) and out of plane (triangles) for Au + Au collisions at centrality 20%–60%. Open symbols are reflections of solid symbols around $\Delta\phi = 0$ and $\Delta\phi = \pi$. Elliptic flow contribution is shown by dashed lines. Lower panel: Distributions after subtracting elliptic flow, and the corresponding measurement in $p + p$ collisions (histogram).

and trigger particles, respectively, and $\langle \cos 2\Delta\Psi \rangle$ is the reaction plane resolution [11]. For the given centrality $\langle \cos(2\Delta\Psi) \rangle = 0.70$; $v_2^{\text{assoc}} = 0.20$, and $v_2^{\text{trig}} = 0.18$, measured via the reaction plane method. For the estimate of the systematic uncertainty in the determination of the flow contribution, we have varied v_2^{assoc} and v_2^{trig} between 0.167 and 0.213 ($v_2\{4\}$ and $v_2\{2\}$ measured in the range $2 < p_t < 6$ GeV/ c). To reduce the systematics, a z vertex cut of ± 25 cm is applied to $p + p$ events to match that in Au + Au events.

The distributions were fit to Eq. (2) in the region $0.75 < |\Delta\phi| < 2.24$ rad, with B as the only free parameter, to determine the amount of background. For the in-plane distribution, $B = 0.649 \pm 0.004(\text{stat}) \pm 0.005(\text{syst})$, and for the out-of-plane distribution, $B = 0.638 \pm 0.004(\text{stat}) \pm 0.002(\text{syst})$. The systematic errors were estimated from using different ranges of $\Delta\phi$ in the fit. We observe a strong excess of two-particle correlations over the correlation pattern generated by elliptic flow in the region $|\Delta\phi| < 0.75$ for both in-plane and out-of-plane distributions, characteristic of nearside intrajet correlations. In the region around $\Delta\phi = \pi$, we observe an excess for the in-plane distribution, but no excess is found for the out-of-plane distribution. This is better illustrated in the lower panel of Fig. 3, where we show the flow-subtracted in-plane and out-of-plane distributions compared to that measured in $p + p$ collisions. The level of combinatorial background measured in $p + p$ collisions, 0.014 ± 0.001 , has been subtracted. The nearside jetlike correlations measured in Au + Au are similar to those measured in $p + p$ collisions.

The back-to-back (around $\Delta\phi = \pi$) correlations measured in Au + Au collisions for in-plane trigger particles are suppressed compared to $p + p$, and even more suppressed for the out-of-plane trigger particles. For the near angle correlations in the relative azimuthal region $|\Delta\phi| < 0.75$ rad, the integrals of the azimuthal distributions are $0.078 \pm 0.014(\text{stat})^{+0.059}_{-0.031}(\text{syst})$ in plane and $0.081 \pm 0.014(\text{stat})^{+0.004}_{-0.021}(\text{syst})$ out of plane. For the back-to-back correlations in the relative azimuthal region $|\Delta\phi - \pi| < 0.75$ rad, the integrals are $0.048 \pm 0.014(\text{stat})^{+0.059}_{-0.031}(\text{syst})$ in plane and $0.014 \pm 0.014(\text{stat})^{+0.004}_{-0.021}(\text{syst})$ out of plane. Note that the large systematic errors in Fig. 3 (lower panel), resulting from the uncertainty in the subtraction of elliptic flow contribution, are highly anticorrelated: assuming weaker (stronger) elliptic flow results in the upper (lower) systematic error bar for $dn^{\text{in}}/d\Delta\phi$ and lower (upper) systematic error bar for $dn^{\text{out}}/d\Delta\phi$ distributions.

A different approach to remove the elliptic flow contribution to the two-particle distributions is to subtract the raw away-side correlations from the near-side correlations measured in the same $|\Delta\phi|$ range (in this case, the elliptic flow contribution cancels out). The difference in the correlation strength, an integral over the $\Delta\phi$ region, on the near side ($|\Delta\phi| < 0.75$ rad) and the away side ($|\Delta\phi - \pi| < 0.75$ rad) is measured to be $0.030 \pm 0.011(\text{stat})$ for the in-plane triggers and $0.067 \pm 0.011(\text{stat})$ for the out-of-plane triggers where the systematic uncertainty due to elliptic flow is canceled out, and the remaining systematic uncertainties are smaller than the statistical errors. Assuming similar strength of the near-side correlations in plane and out of plane, the observed difference can be attributed to the suppression of away-side correlations which depends on the reaction plane orientation.

Although results presented above strongly support the jet-quenching scenario qualitatively, the amount of elliptic flow observed at high p_t for collisions at $\sqrt{s_{NN}} = 130$ GeV seems to exceed the values expected in the case of complete quenching [23]. Extreme quenching leads to emission of high- p_t particles predominantly from the surface, and in

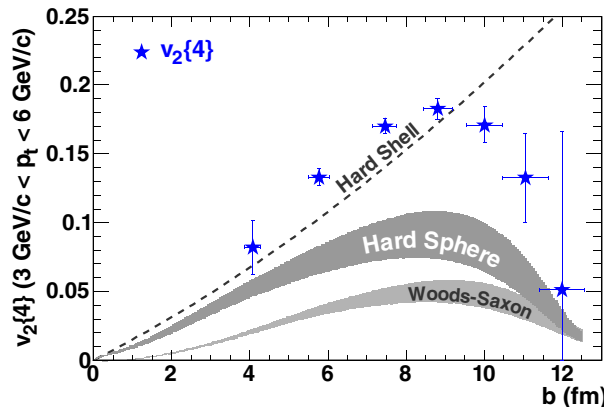


FIG. 4 (color online). v_2 at $3 \leq p_t \leq 6$ GeV/ c versus impact parameter, b , compared to models of particle emission by a static source (see text).

this case v_2 would be fully determined by the geometry of the collision. This hypothesis can be tested by studying the centrality dependence of v_2 for high- p_t particles.

Figure 4 shows v_2 in the p_t range of 3–6 GeV/c (where v_2 is approximately maximal and constant) versus the impact parameter. The values of the impact parameters were obtained using a Monte Carlo Glauber calculation [24]. The measured values of v_2 [4] are compared to various simple models of jet quenching. The upper curve corresponds to a complete quenching, in which particles are emitted from a hard shell [23,25]; this gives the maximum values of v_2 that are possible in a surface emission scenario. A more realistic calculation corresponds to a parametrization of jet energy loss in a static medium where the absorption coefficient is set to match the suppression of the inclusive hadron yields [5]. The density distributions of the static medium are modeled using a step function (following [26]) and a more realistic Woods-Saxon distribution (following [27]). The corresponding v_2 values are shown as the upper and lower bands, respectively. The lower and upper boundaries of bands correspond to an absorption that gives a suppression factor of 3 and 5 [5], respectively, in central collisions. Over the whole centrality range, the measured v_2 values are much larger compared to calculations. Taking into account that this measurement is dominated by the lower p_t side (3 GeV/c), the quark coalescence mechanism [28] might be responsible for the difference, but no quantitative explanation for the observed large elliptic flow exists at the moment.

In summary, we have shown that the charged particle elliptic anisotropy in midcentral Au + Au collisions at $\sqrt{s_{NN}} = 200$ GeV extends to large transverse momenta, at least up to $p_t = 7$ GeV/c, as expected in a jet-quenching scenario. By performing multiparticle correlation analysis and comparing the azimuthal correlations in Au + Au collisions to those in $p + p$, we find the contribution of the effects not associated with the reaction plane orientation is relatively small in midcentral events but could be significant in peripheral and central collisions. We report stronger suppression of the back-to-back high p_t correlations for out-of-plane triggers compared to in-plane triggers, again consistent with a jet-quenching picture. v_2 integrated from moderate to high p_t , approximately in the region where it reaches a maximum, clearly exceeds the limits set for elliptic flow due to a simple jet-quenching mechanism, and still waits for a quantitative theoretical explanation.

We thank the RHIC Operations Group and RCF at BNL, and the NERSC Center at LBNL for their support. This work was supported in part by the HENP Divisions of the Office of Science of the U.S. DOE; the U.S. NSF; the BMBF of Germany; IN2P3, RA, RPL, and EMN of France; EPSRC of the United Kingdom; FAPESP of Brazil; the Russian Ministry of Science and Technology; the Ministry of Education and the NNSFC of China; SFOM of the Czech Republic, FOM and UU of The Netherlands,

DAE, DST, and CSIR of the Government of India; and the Swiss NSF.

-
- [1] See, for example, J. W. Harris and B. Müller, *Annu. Rev. Nucl. Part. Sci.* **46**, 71 (1996).
 - [2] M. Gyulassy and M. Plümer, *Phys. Lett. B* **243**, 432 (1990); X. N. Wang and M. Gyulassy, *Phys. Rev. D* **44**, 3501 (1991); *Phys. Rev. Lett.* **68**, 1480 (1992); R. Baier, D. Schiff, and B. G. Zakharov, *Annu. Rev. Nucl. Part. Sci.* **50**, 37 (2000).
 - [3] PHENIX Collaboration, K. Adcox *et al.*, *Phys. Rev. Lett.* **88**, 022301 (2002).
 - [4] STAR Collaboration, C. Adler *et al.*, *Phys. Rev. Lett.* **89**, 202301 (2002).
 - [5] STAR Collaboration, J. Adams *et al.*, *Phys. Rev. Lett.* **91**, 172302 (2003).
 - [6] STAR Collaboration, C. Adler *et al.*, *Phys. Rev. Lett.* **90**, 082302 (2003).
 - [7] STAR Collaboration, J. Adams *et al.*, *Phys. Rev. Lett.* **91**, 072304 (2003).
 - [8] STAR Collaboration, C. Adler *et al.*, *Phys. Rev. Lett.* **90**, 032301 (2003).
 - [9] R. J. M. Snellings, A. M. Poskanzer, and S. A. Voloshin, *nucl-ex/9904003*.
 - [10] X. N. Wang, *Phys. Rev. C* **63**, 054902 (2001).
 - [11] A. M. Poskanzer and S. A. Voloshin, *Phys. Rev. C* **58**, 1671 (1998).
 - [12] N. Borghini, P. M. Dinh, and J.-Y. Ollitrault, *Phys. Rev. C* **63**, 054906 (2001).
 - [13] N. Borghini, P. M. Dinh, and J.-Y. Ollitrault, *Phys. Rev. C* **64**, 054901 (2001).
 - [14] M. Anderson *et al.*, *Nucl. Instrum. Methods Phys. Res., Sect. A* **499**, 659 (2003).
 - [15] STAR Collaboration, K. H. Ackermann *et al.*, *Nucl. Instrum. Methods Phys. Res., Sect. A* **499**, 624 (2003).
 - [16] STAR Collaboration, K. H. Ackermann *et al.*, *Phys. Rev. Lett.* **86**, 402 (2001).
 - [17] STAR Collaboration, C. Adler *et al.*, *Phys. Rev. C* **66**, 034904 (2002).
 - [18] Y. V. Kovchegov and K. L. Tuchin, *Nucl. Phys. A* **708**, 413c (2002); *A717*, 249c (2003).
 - [19] M. Miller and R. Snellings, *nucl-ex/0312008*.
 - [20] PHENIX Collaboration, S. S. Adler *et al.*, *Phys. Rev. Lett.* **91**, 182301 (2003).
 - [21] CERES/NA45 Collaboration, G. Agakichiev *et al.*, *Phys. Rev. Lett.* **92**, 032301 (2004).
 - [22] J. Bielcikova, S. Esumi, K. Filimonov, S. Voloshin, and J. P. Wurm, *Phys. Rev. C* **69**, 021901(R) (2004).
 - [23] E. V. Shuryak, *Phys. Rev. C* **66**, 027902 (2002).
 - [24] B. B. Back *et al.*, *Phys. Rev. C* **65**, 031901(R) (2002); K. Adcox *et al.*, *Phys. Rev. Lett.* **86**, 3500 (2001); I. G. Bearden *et al.*, *Phys. Lett. B* **523**, 227 (2001).
 - [25] S. A. Voloshin, *Nucl. Phys. A* **715**, 379c (2003).
 - [26] Xin-Nian Wang (private communication). Calculation is based on the framework of *Phys. Lett. B* **595**, 165 (2004).
 - [27] A. Drees, H. Feng, and J. Jia, *nucl-th/0310044*.
 - [28] D. Molnar and S. Voloshin, *Phys. Rev. Lett.* **91**, 092301 (2003).